Application of deep learning in the prediction of benign and malignant thyroid nodules on ultrasound images

Yinghui Lu[1*], Yi Yang[3], Ling Wang1, Qin Li[1], Wan Chen[2]
1.Department of Ultrasound, Zhumadian Central Hospital; Zhumadian Henan , 463000, China
2.Department of Ultrasound Medicine, Shenzhen Hospital of Southern Medical University; Shenzhen   Guangdong, 518100, China

3.Department of Ultrasound，Dongguan City Maternal & Child Health Hospital ; Dongguan Guangdong, 523000, China

Corresponding Author: Yinghui Lu,(E-mail:15989328158@163.com)

ABSTRACT In this paper, ultrasound imaging of benign and malignant thyroid nodules to predict the depth of the learning algorithm, built on circulation volume product thyroid ultrasound image neural network forecasting model. Introduced the convolutional neural network and the recurrent neural network, and combined the advantages of the convolutional neural network and the recurrent neural network, improved the prediction model, constructed the recurrent convolutional neural network prediction model and optimized the prediction model. Soc max algorithm and L2 regularization are introduced to prevent the occurrence of over-fitting. This study introduces the technology and tools required for the development of forecasting systems, the feasibility analysis of the system, demand analysis and system design and other system development preliminary work. Describes the function of the thyroid nodule prediction system and related work such as system testing. Based on the above research, thyroid ultrasound images obtained by the cooperative hospital are used as a data set, and the cyclic convolutional neural network prediction model is used to predict training and testing to the development of a thyroid nodule prediction system. The experimental results show that the prediction system has high prediction accuracy.

INDEX TERMS deep learning; ultrasound imaging; thyroid nodules; benign and malignant prediction.

I. INTRODUCTION

Thyroid nodular diseases are common clinically. It is reported in the literature that nearly 5% of nodules can be found on palpation, and 10% to 67% can be found on ultrasound. Although the incidence of thyroid nodules is high, only 5% to 10% are malignant. Thyroid cancer is the most common endocrine malignant tumor and the fastest growing cancer among all cancers. Thyroid cancer accounts for 1% of all cancers, of which papillary cancer accounts for the majority, and well-differentiated papillary thyroid carcinoma (PTC) accounts for 75% to 90% of thyroid cancer, and the prognosis is relatively good, but the postoperative recurrence rate up to 30% [1]. Because thyroid cancer progresses relatively slowly, some research related to its diagnosis has been completed, and early thyroid cancer may be cured. Non-invasive can provide necessary diagnostic information for potentially malignant thyroid nodules, and is regarded as a valuable diagnostic method in clinical practice. It proposed that high-resolution ultrasound is currently the preferred method to assess the nature of thyroid nodules, and it can no longer only distinguish the cystic and solid nodules, but also plays an important role in distinguishing benign and

malignant nodules [2-3]. Ultrasound has become the preferred examination method for evaluating the nature of thyroid nodules due to its practicality, low cost, no discomfort for patients, and no radiation. Ultrasound can also be found in addition to a palpable nodule, nodule size is estimated, the volume of goiter, and guide fine-needle aspiration biopsy (FNAB) [4]. Careful analysis of the main topographic features of thyroid nodules can help clinicians select nodules for further FNAB examination. FNAB has been shown to increase the positive rate of diagnosis and is essential for biopsy of more and more small nodules [5].

In the conventional CAD mainly rely on the computer to emulate biological neural processes information. The method first needs to artificially extract the morphological and texture characteristics of the lesion in the image, and then use a large amount of data to train it [6]. It evaluated the diagnostic potential of the six tumor markers involved in the design of ANN in the auxiliary diagnosis of lung cancer. It performed well in the differentiation of lung cancer from benign lung diseases and the other three types of gastrointestinal malignancy. We used in traditional ANN to classify liver fibrosis non-invasively with an accuracy of

IEEE *Access*

88.3%. Doctors can refer to the results to diagnose and treat patients [7]. It reduced the pain and the risk of various complications caused by invasive examinations. In the identification of thyroid nodules, it used feature extraction methods to train artificial neural networks for thyroid nodules, and the accuracy of their diagnosis was more than 80% [8]. At present, the most widely promoted commercial CAD is AmCAD-UTDetection, which has an AUC of 0.88 in the risk stratification of thyroid nodules. However, this method has obvious disadvantages. In terms of structure, the ANN structure is relatively simple, with only 1 to 2 hidden layers [9]. In terms of usage methods, this method generally only has a diagnostic function and cannot automatically locate the lesion. Before detecting the nature of the lesion, it is necessary to manually outline the lesion. In terms of feature extraction, all features need to be extracted manually. This places high requirements on diagnosis and detailed observation for disease diagnosis doctors and software developers, and the process is expensive [10-11]. It is time-consuming and prone to feature omissions and bias so that the features of the image cannot be fully explored. Although this method improves the accuracy, there is still a problem, that is, the phenomenon of overfitting is serious [12]. It proposed a new computer-aided detection system for lung nodules using a multi-view convolutional network. Three people previously developed candidate detectors for lung nodules are combined in a 3D chest CT scan, and then 2D plaques centered on these features are extracted in nine different directions. Finally, different convolutional neural networks are used. Combined with prediction, the accuracy rate reaches 85.4% [12]. The method mentioned in this article provides new ideas for the prediction of thyroid ultrasound images of deep convolutional neural networks such as AlexNet, VGG, GoogLeNet, and ResNet. In the ultrasound diagnosis of thyroid nodules, Ma et al. Improved the CNN model and used a multi-view strategy to segment the thyroid nodules with an accuracy rate of 91.5%. It can accurately depict the boundaries of the nodules in the ultrasound image [13]. A good replacement for time-consuming and tedious manual segmentation methods. The CNN model is based on discrete wavelet transform features to predict thyroid nodules with TI-RADS, and its accuracy is 98.9%~100%. Kewei improved the FasterR-CNN network model so that the true positive rate of the model for the diagnosis of papillary thyroid carcinoma reached 88.8%.

According to the above information, the accuracy of using convolutional neural networks to diagnose thyroid nodules is higher than that of traditional artificial neural networks, but there is still room for improvement in the accuracy of thyroid nodule positioning or diagnosis accuracy [14]. There is a lack of a deep learning network target detection model that can locate and diagnose nodules at the same time. Therefore, this research tries to build an excellent target detection model for the diagnosis of thyroid benign and malignant nodules [15]. The constructed detection model is the same as the current mainstream target detection model and the diagnostic value of high-age ultrasound diagnosticians based on the thyroid imaging data reporting system in the differentiation of benign and malignant thyroid nodules.

II. DEEP LEARNING PROCESSING DESIGN FOR ULTRASOUND IMAGES

A. Improved CascadeMaskR- CNN thyroid nodule detection network

The detection model constructed in this experiment is improved based on the advanced CascadeMaskR-CNN model in the detection field. Unlike most detection models, where the positioning and qualitative of the target detection object are in series, positioning, and qualitative of CascadeMaskR-CNN is performed in parallel in parallel. The detection quality of natural images and some specific things are relatively high, but the characteristics of thyroid nodules of different nature in ultrasound images are not clear, so the model has low accuracy in positioning the position of thyroid nodules [16]. The accuracy rate is low. Therefore, this research is based on its improvement. CascadeMaskR-CNN originally presented the features obtained after ROIAlign processing the image to a detector composed of two fully connected layers to complete the prediction and regression tasks. This study replaced the two fully connected layers with five convolutional layers and a fully connected layer, as shown in Figure 1. The shallower convolutional layer can learn local features in a small range [17]. The deeper convolutional layer can learn more abstract features a large range, and the multi-layer convolutional layer can improve the recognition performance of the model. The features are obtained after the previous step is first presented to the convolutional layer to further explore the hidden features, and then presented to the fully connected layer.
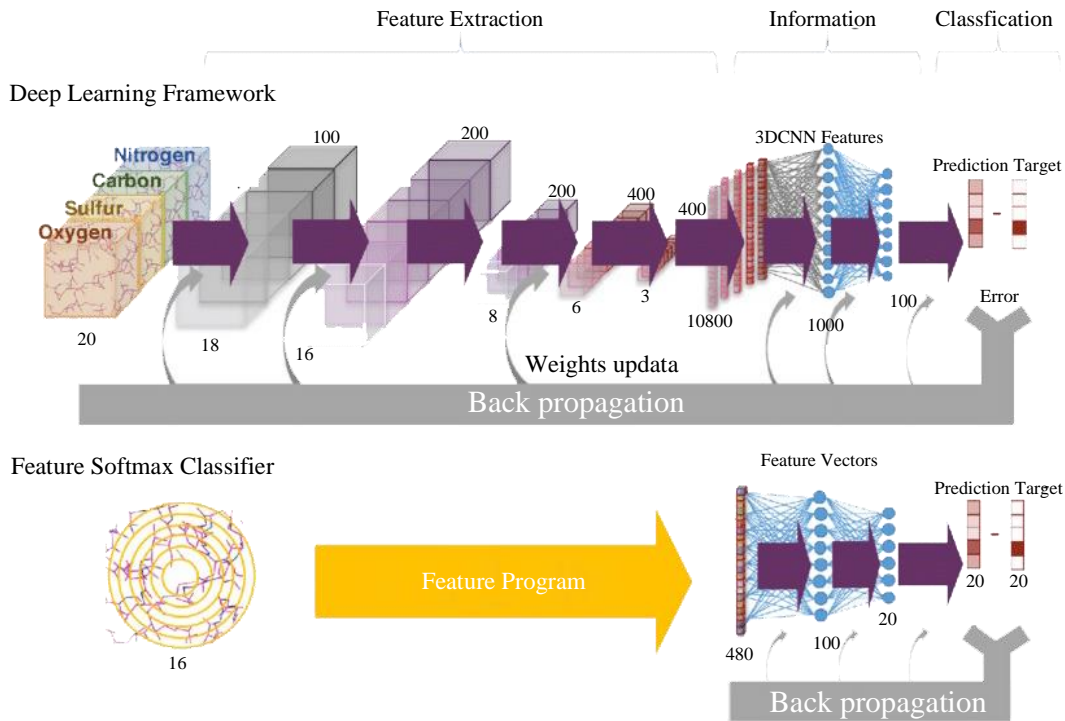
FIGURE 1.**Two detector architecture**

The formula is used to increase the gradient value of the accurate sample. The parameter is used to ensure that under the condition of Lb, the function in the two cases in the following equation is continuous. This function solves the problem of imbalance between the objective function prediction task and the positioning task during the training process and further improves the performance of the model.

$$K_b(x) = \begin{cases} \dfrac{a}{b}\big(b|x|=1\big)\ln\big(b|x|=1\big) \\ \gamma|x|+C \end{cases} \quad （1）$$

$$\gamma = \alpha\ln(b+1) \quad （2）$$

The basic unit multiplexing is a cyclic neural network. A cyclic neural network composed of basic units. The weight matrix calculated by each layer of the network will be input to the lower network structure. The t represents time, x represents the input of the network, O represents the output of the network, and S represents the weight matrix of the upper network. Using the activation function, the cyclic neural network can be defined as:

$$\mathrm{D}_t = f(u^*x + w^*D_{t-1}) \quad （3）$$

The basic unit is combined and refused to complete the main work content of the cyclic neural network. The forget gate decides to discard and retain the information. This layer will output a value between 0 and 1 to the neuron to decide whether to retain it.

$$F_t = f(u_t^*x + w^*D_{t-1}) \quad （4）$$

The cyclic neural network is based on the LSTM network, and its parameters are adjusted and optimized for the network model of this paper. Among them, the forget gate

reads the output of the upper unit and the input of the current unit and outputs a value between 0 and 1 to each neuron, and the neuron decides the content of the choice. The activation function is generated by an input gate to prepare for updating network data. The output gate processes the output information of the sigmoid layer through the activation function and outputs the final information. The network as a three-time recurrent neural network, connected with the statement commonly used in the mining direction relationship between samples and the like features to achieve a correlation between the sample with the features of a thyroid ultrasound image in the present study, followed by reduction of the clinical symptoms of the disease relationship between [18].

Non-maximal suppression (NMS) is not inhibited the element. Through this method, find the local maximum value and suppress other values in the neighborhood. In target detection, in order not to miss any detected targets, the model often outputs frames far exceeding the actual number of detected targets, and there will be a considerable number of frames that are roughly the same, in a contained or crossed the state to frame the same target. Each frame has a confidence level, and the role of NMS is to select the best one among the stacked frames [19]. The NMS can select the frame with the highest confidence level, while suppressing the low-confidence frame, and set the confidence level of the low-confidence frame to 0 to remove it. This method can reduce the workload of subsequent data processing. But when there are multiple target detection objects in the same image, this method will affect the detection. The score reset function of NMS is as follows:

IEEE *Access*

$$R_i = \begin{cases} R_i, iou(M,b_i) < N_t \\ 0, iou(M,b_i) \geq N_t \end{cases} \quad （5）$$

However, the soft-NMS algorithm sets an attenuation function for adjacent detection frames. When the confidence of some detection frames is low, this method prevents the confidence of the frame from becoming 0. When a real target is within the preset overlap threshold, the situation that the target may not be detected is avoided. The soft-NMS function is as follows:

$$R_i = S_i e^{-\frac{iou(M,b_i)^2}{\sigma}}, \forall b_i \notin D \quad （6）$$

In the training process of CNN, only a sufficiently large data set can meet its training requirements. However, for medical target detection models, it is usually difficult to obtain such a large number of high-quality training samples in a short period. Therefore, the progress of CNN has certain limitations in medical imaging. The model in this experiment uses ResNet-101 for image feature extraction, which itself has a very good ability to recognize natural images, but its performance in the recognition of ultrasound images of the thyroid is not ideal, and this experiment can provide The pictures are limited, which limits the training of the network. Transfer learning can overcome this problem by applying well-trained deep models to other image data sets for feature extraction.

B. Data source design for thyroid nodules

Among them, local data containing negative thyroid ultrasound image 719 sheets, positive thyroid ultrasound image 367 sheets, a total of 1086 Zhang. In the thyroid ultrasound image database proposed by Romero, 357 pieces were marked as positive data and 71 pieces were marked as negative data, a total of 428 pieces. The thyroid ultrasound image classification used in the experiment was carried out according to the doctor's guidance and combined with the TI-RADS evaluation standard [20]. This experiment is in benign and malignant thyroid nodules forecast predicted based on the malignant nodules do fine-grained forecast predicts that the patient can make more detailed. The prediction of normal thyroid and thyroid with the nodular disease, on the one hand, provides a reference for the fine-grained prediction of thyroid benign and malignant and malignant. On the other hand, it provides the basis for subsequent time-series disease development predictions for patients. After the ultrasound image is processed according to the image processing method, it is divided into three groups of data, as showed in Table 1.

TABLE 1
Training data of thyroid prediction model

		Local	Romero E	total
Classification I	Normal	2591	430	2177
	nodule	1305	245	1203
Classification II	Benign	609	274	843
	Malignant	487	743	1277
Classification III	Malignant	285	598	845
	Exterior	276	589	863

We inquire about the basic medical history of patients who found thyroid nodules during thyroid ultrasonography. If the patient has no history of thyroid surgery or neck radiotherapy or chemotherapy, gray-scale ultrasound images of the thyroid nodules will be collected. During the acquisition process, the patient lay down, with the head tilted back, and the neck was fully exposed so that the thyroid nodules were displayed clearly and completely in the ultrasound image, and normal thyroid tissue could be seen around the nodules [21]. We measure the maximum diameter of the nodule in cm and record it, and collect ultrasound images for each module according to the actual situation. It records basic information about the patient's gender, age, and pathology follow-up, excluding cross- border and no pathological tumor patients [22]. In the end, 203 nodules from 177 patients were included in this experiment.

They are the normal data group, benign nodules-malignant nodules data group, nodule preliminary deterioration-nodule height deterioration data group, these three sets of data are used as three prediction experiments. Among them, local and Romero are respectively the amount of data used in the experiment after the processing of local data and images published on the Internet by Romero and others, and the total is the total amount of data in the data set, that is, the sum of local data and RomeroE data [23]. Data grouping is based on the combination of the guidance of the chief physician of the partner hospital and the TI-RADS evaluation criteria. In the TI-RADS evaluation standard, malignant nodules include several TI-RADS grades, and the severity of malignancy is divided into two categories, which is an indicator of fine-grained malignant nodules, as shown in Figure 2.
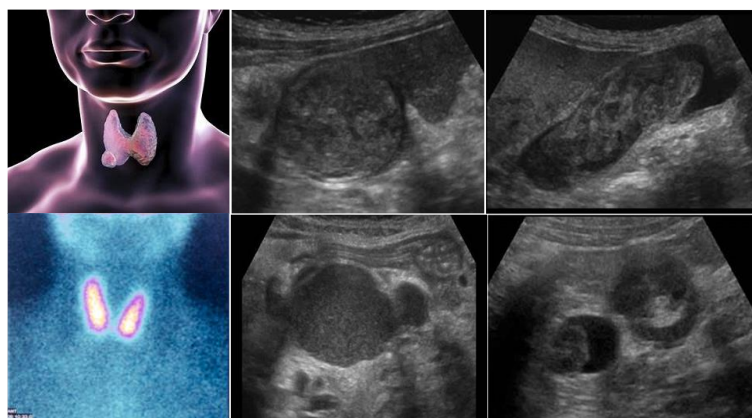
IEEE *Access*

FIGURE 2.**Example of thyroid nodule data**

The picture can be cut to make full use of the image on the premise that the thyroid nodule and its surrounding normal tissue and structure can be fully displayed. Thyroid nodules in all pictures are marked with the module position and benign and malignant nodules [24]. This process is completed by a stenographer with rich experience in diagnosing thyroid nodules using the annotation software. The labeling process uses the VIA tool to draw a polygonal box to surround the thyroid nodule and generate a son format file for training the model [25]. After the work is completed, another experienced stenographer will review one by one to ensure the accuracy of the above work. Desensitizing the data plays a role in protecting sensitive patient information, so it is of great significance in the prediction and prediction of thyroid ultrasound images. The text data obtained in this article contain sensitive information such as the patient's name, gender, and date of birth [26]. The image data includes hospital information, imaging equipment information, patient examination information, and so on. On the one hand, removing these contents reduces the interference to the experiment, on the other hand, it can conceal sensitive patient information. Common covert data have established internet desensitization, used in this experiment was a simple manner, the encrypted sensitive patient information table into the child table, sensitive information thyroid ultrasound image using shielded manner. The exclusion criteria were a history of thyroid surgery and a history of radiotherapy and chemotherapy in the neck [27]. Thyroid nodules were too large to show normal thyroid tissue. The pathology of the thyroid was a borderline tumor, and thyroid nodules had no pathological results.

III. DESIGN OF PREDICTION METHOD FOR BENIGN AND MALIGNANT THYROID NODULES

A. System design and implementation

We analyze and design the thyroid nodule prediction system, and make a detailed analysis in terms of feasibility to prove the feasibility of the development of the thyroid nodule prediction system, sort out user needs, and analyze and design the overall architecture of the system according to the demand analysis. Then the database data storage

method and structure are designed in detail. According to the design idea of this thyroid nodule prediction system, the realization of system function is explained. The homepage of the system introduces the system, the function part of the acquisition, processing, and prediction of thyroid ultrasound images [28]. To ensure the correctness and completeness of system functions, software testing methods are used to perform functional tests on the system to pave the way for the system to go online.

In the process of information software system development, the most important key to determining the success or failure of an information system is system analysis [29]. The key to system analysis is to clarify the tasks of the information system. The problems to be solved are mainly for the main tasks of the information system. It realizes the technical choice of the system. It determines the system model, write the corresponding development files, construct the system use case diagram, etc., and clarify the specific implementation process of the system, and then formulate the work breakdown structure, and make detailed plans for the system implementation.

The focus of the software information system is to do a detailed information system feasibility analysis [30]. The feasibility analysis needs to start from different angles, mainly considering technical feasibility analysis, operational feasibility analysis, economic feasibility analysis, environmental feasibility analysis, etc. The development of this project follows the development process of software engineering, and comprehensive feasibility analysis of system development is done. The thyroid nodule prediction system has low hardware requirements for customers and developers [31]. Users only need to have a network connection and any terminal device that can use a browser, by operating the web page displayed to the user. We can use system functions, developers need ordinary PC machines will be able to complete the development of this system. The development and testing of the thyroid nodule prediction system all use normal browsers, and the development and testing can be completed using Windows or Linux systems. The system is easy to operate, simple, and easy to learn, the system interface design is simple, convenient, high interpersonal interaction, and there is no theoretical

requirement for the user's computer level. The development goal of the thyroid nodule prediction system is clear, and the technical tools used are mature [32]. The development of this system is feasible.

Because of the clinical diagnosis of thyroid nodules is easily affected by doctors and other factors, diagnosis defects are prone to appear in clinical diagnosis. The purpose of the development of the thyroid nodule prediction system is to improve the accuracy and efficiency of diagnosis and prevent the influence of many unfavorable factors. At present, the medical level development in the east and west is extremely unbalanced, and the medical level in the central and western regions is relatively backward. In the clinical diagnosis of thyroid nodules, it is more susceptible to the influence of many factors than in the eastern region, causing

diagnostic errors. The development of this system can not only improve the prediction accuracy of thyroid nodules, avoid the subjective wishes of doctors, improve diagnosis efficiency, and reduce the rate of misdiagnosis, but also improve the medical level of the central and western regions and weaken the differences between the east and the west. Thyroid nodules forecasting system has clear objectives, after the technical feasibility, operational feasibility, economic viability and environmental feasibility of doing a detailed analysis concluded [33-34]. This system has high feasibility of development, not only in actual use Improve the level of medical care, and patients with thyroid disease are the main beneficiaries. Therefore, it is generally feasible to develop a thyroid nodule prediction system, as shown in Figure 3.
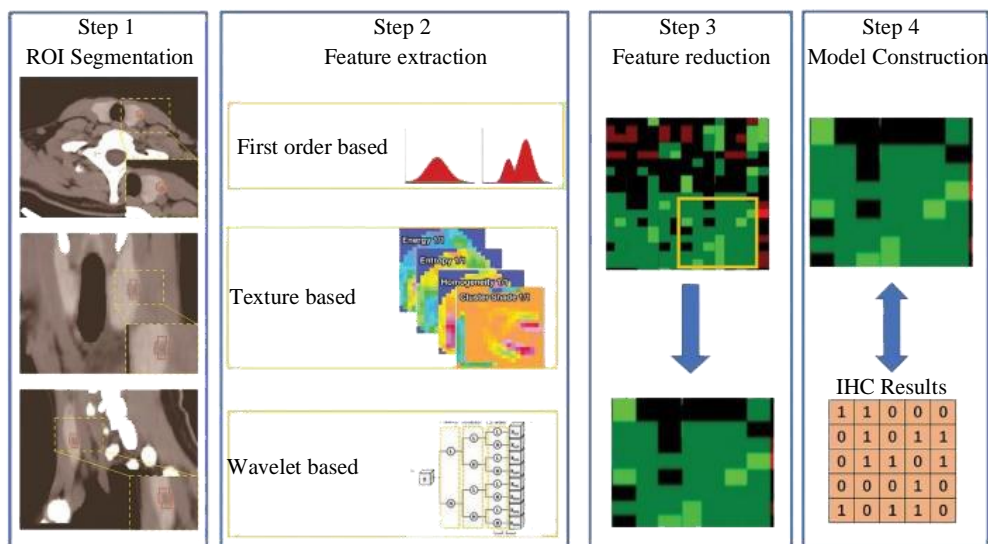

FIGURE 3. **Main function diagram of the thyroid prediction system**

This thyroid nodule prediction system is mainly divided into a browser part, a web server part, a business logic part, and a database part. This system is constructed based on the B/S structure of the webserver and the browser. The system is divided into four layers, four layers include a model layer, data access layer, business logic layer, view layer. The development of the thyroid nodule prediction system follows the standardized development requirements for data manipulation and business logic implementation. The model layer is mainly to encapsulate the tables in the database as objects so that the processing results such as database data reading and logical business are stored in the database. The data access layer encapsulates operations such as adding, deleting, modifying, and checking database data, and other modules call the interface provided by this module to implement operations on database data. Maintaining system data access and object persistence is the main task of the data access layer [35]. By encapsulating the database data operation method, not only can the data be accessed and processed safely, but also the efficiency of database access can be improved. The business logic layer is to encapsulate the logic processing process that realizes various functions and realize the interaction between the integrated view layer,

the model layer, and the data access layer. It is the core of the entire business processing process and has the main position of multiplying up and down. The view layer is the interface through which the user uses the system through the intermediary, and is an important component for the perfect interaction between the user and the system. The main function of this layer is displayed [36]. The layer is used to display all the functions of the system, and the user needs through this layer. The business is submitted to the webserver for the HTTP protocol, and the business processing is realized.

B. Evaluation of index design

In this study, the average accuracy was used to evaluate the positioning performance of the model. Among the nodules accurately located by the model, this study defines malignant nodules as positive samples and benign nodules as negative samples. When the model judges a malignant nodule as malignant, it is a true positive. When a benign nodule is judged as negative, it is truly negative. When a malignant nodule is judged to be benign, it is a false negative. When a benign nodule is judged to be malignant, it is a false positive. We compare the improved CascadeMaskR-CNN

target detection model in this experiment with the initial CascadeMaskR-CNN target detection model and the improved FasterR-CNN target detection model mentioned in the introduction. We use the remaining 281 thyroid ultrasound images as a test set and import 3 models to detect

whether the model's ability to locate and diagnose thyroid nodules in ultrasound images is improved based on the original model, and how this model compares with other models The performance difference is shown in Figure 4.
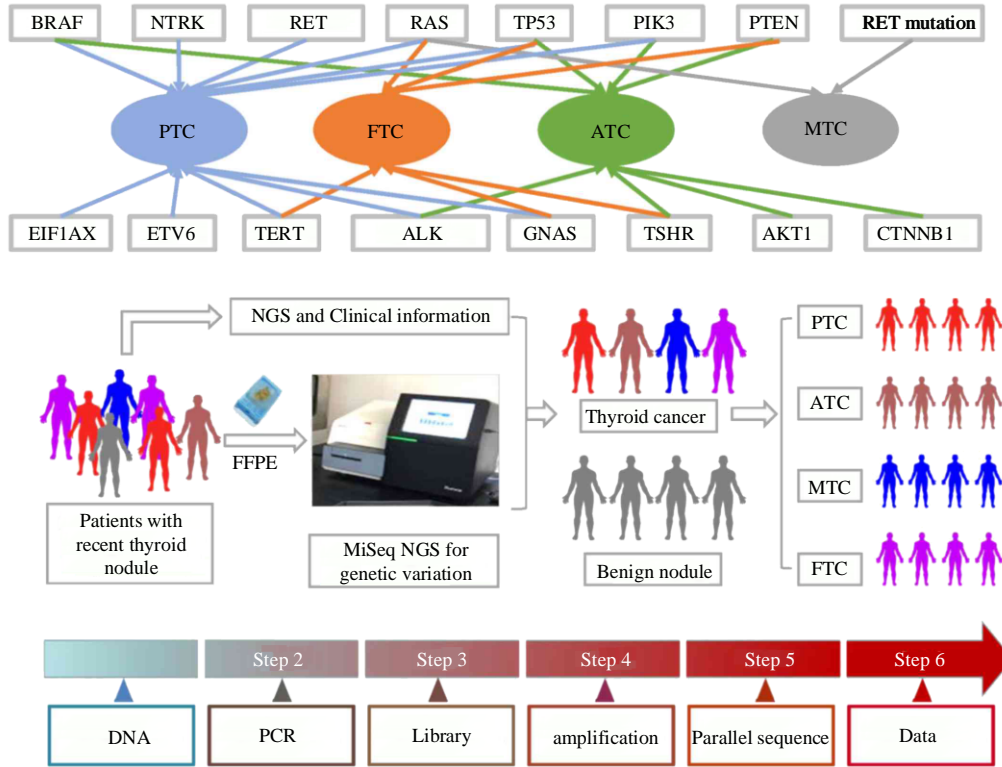

FIGURE 4. **Evaluation steps**

Two senior doctors collaborated to review the above 203 nodules through the workstation without knowing the pathological results, and compare with the pathological results to calculate the best node value for the system to distinguish benign and malignant thyroid nodules. Two doctors predict nodules independently of pathological results based on the Kwak version of TI-RADS and based on the best results obtained from the above-mentioned senior doctors and pathological comparisons the node value classifies the nodule as benign or malignant [37].

Choosing appropriate experimental evaluation indicators is of great significance for testing the performance of the experimental method. This paper uses accuracy and loss function value as the experimental indicators for detecting malignant nodules in thyroid ultrasound images. In the detection results, the false detection as a preliminary deterioration image are defined as true positive (TP) and false-negative (FN), true negative (IN). False-positive (FP), the detection accuracy rate is:

$$A = \frac{1}{n}\sum_{i=1}^{n}\frac{TP+TN}{TP+FN+TN+FP}\times 100\% \quad (7)$$

Sensitivity is calculated as the share of true positives in the sum of the number of true positives and false negatives.

Sensitivity refers to the proportion of thyroid nodule detection experiments that correctly predict the image of malignant nodules. The calculation formula is:

$$S = \frac{TP}{TP+FN} \quad (8)$$

The specificity calculation method is the occupancy rate of true negatives in the sum of the number of true negatives and false positives. Specificity refers to the proportion of thyroid nodule detection experiments that correctly predict the image of benign nodules. The calculation formula is:

$$Sp = \frac{TN}{TN+FP} \quad (9)$$

Loss function values show convergence performance of the network when the network Loss when the functional value of the area is smaller than the numerical value representative of a stable network.

Using SPSS22.0 statistical software for statistical analysis to pathology results as the gold standard, using receiver operating characteristic (ROC) curves obtained by TI-RADS diagnosis of benign and malignant thyroid nodules optimal diagnosis point. It used this value to calculate the results of the diagnosis of benign and malignant thyroid nodules by doctors with high and low experience. The X2 test compares

the sensitivity and specificity of the best node value between high and low experience doctors in distinguishing benign and malignant nodules. The difference is statistically significant. It calculated the mAP of the three target models, the sensitivity, specificity, positive predictive value, and negative predictive value of the three target detection models, senior and junior doctors to diagnose thyroid nodules. It drawed the ROC curve of this target detection model and the comparison ROC curve of the above-mentioned doctors.

IV. RESULTS AND ANALYSIS

A. Analysis of model comparison results

The mAP values of the three models are shown in Figure 5. It can be seen that the improved CascadeMaskR-CNN is better than the CascadeMaskR-CNN and the improved FasterR-CNN in each mAP value. The sensitivity, specificity, positive predictive value, negative predictive value, and accuracy of the three models for diagnosing benign and malignant thyroid nodules can be seen in Figure 6. From the comparison of the values based on the improved FasterR-CNN and CascadeMaskR-CNN basic models, it can be seen that it improved FasterR-CNN except the negative predictive value is higher than the basic model of CascadeMaskR-CNN, which are 0.914 and 0.901, and the other values are all lower than the basic model of CascadeMaskR-CNN. The values of the improved CascadeMaskR-CNN are higher than those of the CascadeMaskR-CNN model.
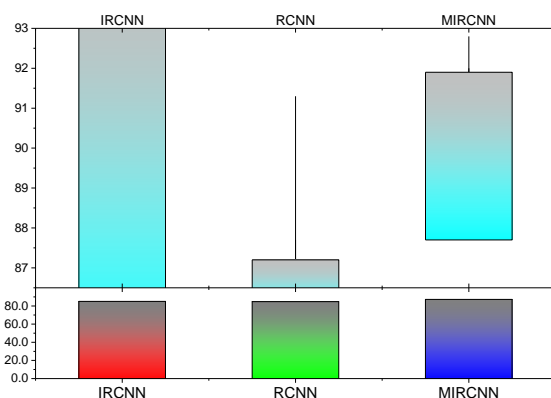

FIGURE 5.**Comparison of mapping values of the three models and comparison of various values of the three models**

According to the ROC curve drawn by senior doctors to diagnose benign and malignant thyroid nodules, the best node value for diagnosis is 3.5, which is between TI-RADS 4b and 4c. Its sensitivity is 0.889, specificity is 0.824, and AUC is 0.894. To improve the specificity of diagnosis and reduce the rate of misdiagnosis, this study defines the node value as 4c, that is, in the subsequent evaluation of junior doctors, the 2/3/4a/4b nodules are regarded as benign, and 4c/5 is considered that nodules are considered malignant. The ROC curve chart compares the diagnosis results of senior and lower senior doctors. The diagnostic efficiency based on the improved CascadeMaskR-CNN model is shown in Figure 6. The sensitivity, specificity, positive predictive

value, negative predictive value, and accuracy rate of senior doctors for nodule diagnosis are higher than those of younger doctors. Among them, the difference in sensitivity between the two was statistically significant, and the difference in specificity between the two was not statistically significant. The accuracy of the improved CascadeMaskR-CNN model are higher than those of senior doctors. The diagnostic efficiency of senior doctors for benign and malignant thyroid nodules is better than that of junior doctors. Diagnostic efficiency of detecting benign and malignant thyroid nodules in the model is better than that of senior doctors.
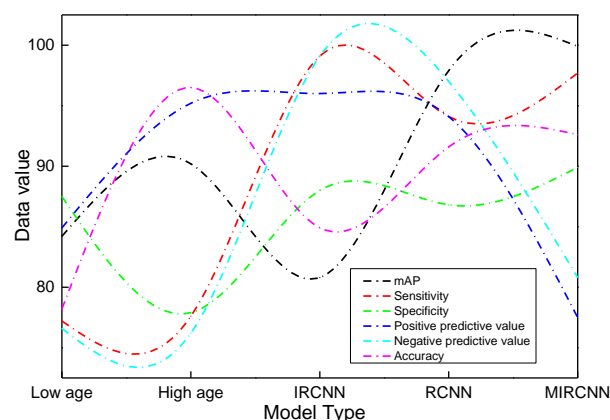

FIGURE 6.**Comparison of the diagnostic efficiency of the improved CascadeMaskR- CNN model among senior and lower-skilled doctors**

To evaluate whether a target detection model is excellent, it mainly depends on two parts. One is the positioning ability of the model, and the other is the qualitative ability under the premise of accurate positioning. In this target detection, the model correctly diagnoses benign and malignant thyroid nodules.

The evaluation of the positioning capability of this model is done through mAP. The so-called localization ability is the ability of the target detection model to correctly find the position of the nodule in the ultrasound image. Currently, mAP is a measure of the performance of target detection models. In this study, the mAP of the three experimental models was all lower than 90%. Compared with their ability to diagnose nodules, this result is slightly inferior. Therefore, the reasons that affect mAP are worth exploring. Reviewing the experimental results, several main reasons affect the model mAP value. The model locates the module but the diagnosis is wrong. The model locates non-nodular tissues as nodules. The model did not locate any suspicious organization, that is, no detection target was found. Since the three models used for comparison in this experiment have a very high accuracy in the diagnosis of benign and malignant thyroid nodules, the mapped value can indirectly represent the ability of the three models to locate modules. The higher the positioning ability, the higher the mAP higher. In this experiment, based on the improved FasterR-CNN, the CascadeMaskR-CNN of mAP values were 80.3%, 84.6%, 87.1%, from mAP values can be learned, CascadeMaskR-

IEEE *Access*

CNN itself image localization The ability is higher than that based on the improved FasterR-CNN, which proves the superiority of the selected detection model this time. Based on the improved CascadeMaskR-CNN, the mapped value of CascadeMaskR-CNN is increased by 2.5% based on CascadeMaskR-CNN, indicating that this experiment has a positive effect on the improvement of the model, and the model image positioning ability has been improved to a certain extent, as shown in Figure 7.
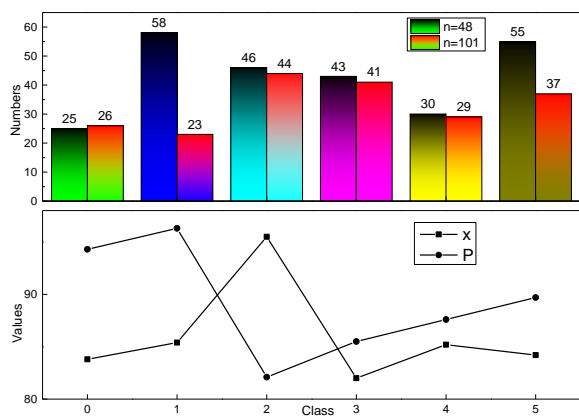

FIGURE 7.**Features of benign and malignant nodules with contrast-enhanced ultrasound**

In terms of the diagnostic performance of the model, the calculation of various values in this study is based on the premise that the model is correctly positioned to the nodule, so the incorrect positioning is discarded [38]. The obtained results on this premise, the model's diagnosis of benign and malignant thyroid nodules accuracy, based on improved CascadeMaskR-CNN higher than the initial CascadeMaskR-CNN than based on improved FasterR-CNN. Firstly, the superiority of the selected model is proved. Regarding the problem that the diagnostic accuracy rate of the improved FasterR-CNN in this study is 92.8% and that of Coway's study is 88.8%, the difference may come from the training set and test differences in the set and slight differences in model construction. Based on the improved CascadeMaskR-CNN, the various values of the thyroid nodules are significantly improved compared to the CascadeMaskR-CNN, and the diagnostic accuracy is increased by 3.2%, indicating that the diagnostic performance of this model for thyroid nodules is better than the original under the premise of correctly positioning the nodules. The model has been fully improved, as showing in Figure 8.
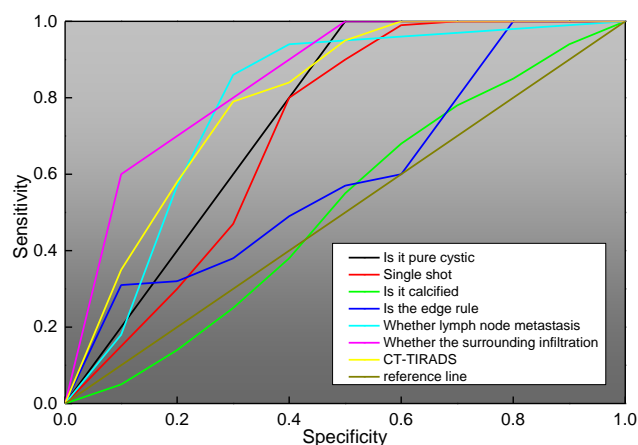

FIGURE 8.**Differentiation of benign and malignant thyroid nodules**

Due to the clinical controversy regarding the best diagnostic threshold of TI-RADS, in this study, two senior doctors strictly followed TI-RADS to predict thyroid nodules and calculated TI-RADS to diagnose benign and malignant thyroid through ROC. The best diagnostic cut-off value for nodules is to classify modules of type 2, 3, 4a, and 4b as a benign group, and classify nodules 4c and 5 as a malignant group. It is used to calculate the diagnostic efficiency of TI-RADS. According to this study, the diagnostic efficiency of high and low-level physicians is higher than 80%, indicating that TI-RADS has high reference value for the diagnosis of thyroid nodules in the clinical application process. However, senior doctors have a larger AUC area in the diagnosis of benign and malignant thyroid nodules, which is higher than that of inexperienced doctors with less seniority, and the diagnostic efficiency is better. It shows that in the actual application of TI-RADS, there is a certain degree of subjectivity among diagnosticians, and the diagnostic efficiency of doctors with lower seniority is slightly worse, as shown in Figure 9.
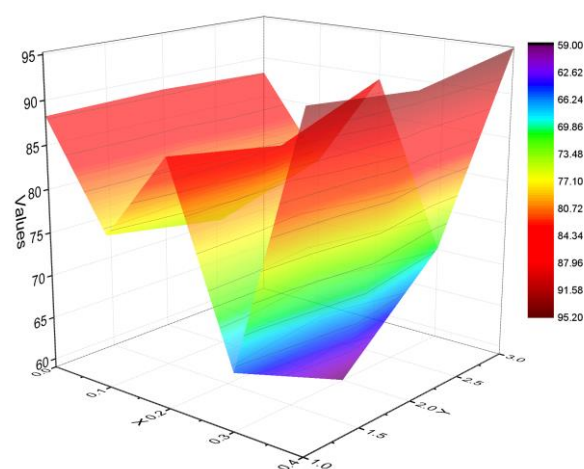

FIGURE 9.**Comparison of prediction results of good and evil thyroid nodules**

The negative predictive value for the diagnosis of thyroid nodules by senior and lower-skilled doctors is lower than the

positive predictive value. The negative predictive values of the two are 0.782 and 0.676 respectively, which are the same as previous research results, indicating that thyroid cancer exists in manual diagnosis Higher missed diagnosis rate. Among them, 5 cases were combined with Hashimoto's background and were in the study with Li Tingting the missed diagnosis of malignant thyroid nodules by ultrasound diagnosticians is roughly consistent. Since TI-RADS4b type thyroid nodules have a malignant probability of about 31%~60%, it is a major difficulty in the differentiation of benign and malignant thyroid nodules. When nodules are encountered in the diagnosis work, they usually need to be combined contrast-enhanced ultrasound or ultrasound electrograph and other tests are used to assist in the diagnosis of such nodules. However, in the detection of the target model, the negative predictive value was 0.968, and only 4 cases of malignant nodules were missed, which showed the superiority of the diagnostic efficiency of this model [39].

The method proposed in this paper has higher sensitivity and specificity for prediction and prediction of thyroid ultrasound images than other prediction methods, and it is concluded that a greater proportion of nodules are detected in the prediction and prediction of thyroid ultrasound images. The prediction effect of the method in this paper is the best. The reason is that the time series features are introduced. The relationship between image features is established while the image features are extracted, which restores the relationship between the clinicopathological features of thyroid nodules to a certain extent. The relationship between the features is reproduced in the form of the association relationship between the image features, and the differences and connections between the image features are fully considered, which improves the adaptability of the predictor, and thus the prediction accuracy rate is higher.

B. Index evaluation results

Introducing a cyclic network model characteristics, prediction predictive capacity significantly increased. The characteristic of traditional convolutional neural network is to extract the image features of thyroid ultrasound images. The method in this paper introduces time series on this basis, so that the network has a certain memory function. After the image features are extracted, the correlation between image features is sorted out, and the thyroid gland is restored. The relationship between clinicopathological characteristics of nodules can achieve highly accurate prediction and prediction.

In addition, in order to verify the fine-grained prediction effect of the cyclic convolutional neural network model in this paper on predicting the more difficult thyroid malignant nodules, experiments were performed on the three data sets produced in this paper. In this experiment, some network parameters in the cyclic convolutional neural network are also set as follows. We set the ReLus function as the activation function, the weight attenuation is 0.0005, and the epoch is 10. The given parameters are consistent with the

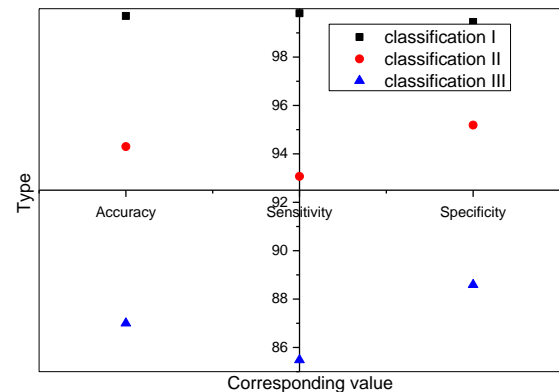experimental environment, the prediction experiment is carried out.

FIGURE 10. **Three-level prediction experiment results**

As shown in Figure 10, the accuracy of prediction between normal thyroid ultrasound images and nodular thyroid ultrasound images is as high as 99.70%. The accuracy rate of prediction of good and bad thyroid nodules exceeded 90% and reached 94.30%. The accuracy of fine-grained prediction of malignant thyroid nodules is as high as 87.00%. The experimental results show that the network prediction model in this paper is superior in the fine-grained prediction of more difficult malignant thyroid nodules. The construction and use of the CNN-Fusion network enhance the network's prediction and prediction ability and network robustness. The network combines thyroid ultrasound images information such as the relationship between features and features is highly fused so that the prediction and prediction network knows image features and their relationships. Compared with the case of only grasping image features and no relationship between features, the relationship between clinical-pathological features cannot be restored to the greatest extent, and then CNN -Fusion constructed using enhanced prediction. Malignant nodules grained prediction (classification) to 87.00% further malignant nodules achieve high accuracy of the predicted prediction, the same test sensitivity, and specificity above 85%. Although classifications accuracy, sensitivity, and specificity than classification and classification low value, for forecasting more difficult and malignant nodules fine-grained prediction results can be achieved at present effect, sufficient to show the circular convolution neural network of networks to predict the effect has superiority. In the experiment, for different predictions during the experiment, the loss value changes were counted to verify that the network has a better effect in this experiment.

As shown in Figure 11, the relationship between the change curve of the accuracy of the three groups of experiments and the number of iterations of the training neural network and the relationship between the loss value curve and the number of iterations of the training neural network are recorded.
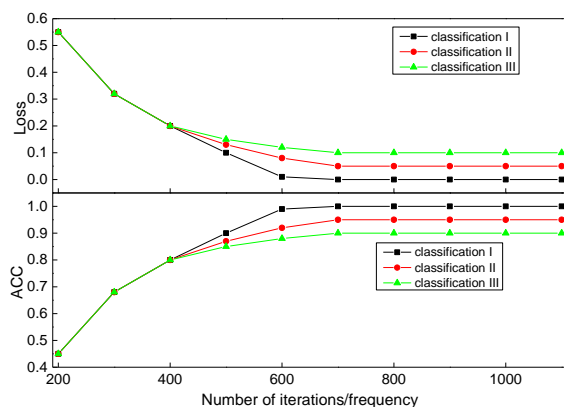
IEEE *Access*

FIGURE 11. **Data diagrams of three-level prediction experiment**

As shown in Figure 11, the accuracy of the three experiments curve, showed increases in the accuracy of the number of iterations. By observing the change curve of the number of iterations and loss value, it is concluded that the model converges faster. After 500 iterations of training, the loss value of all experiments is reduced to 0.3 to scare, the training continues, the loss value is maintained between 0.1-0.2, the predictor has good adaptability, convergence speed, and convergence ability. The network model adopts parameter sharing and local perception to reduce network complexity. The introduction of L2 regularization can effectively avoid network training over-fitting, and the ability to extract features is better.

To verify the optimization effect of the prediction model, based on the introduction of L2 regularization, the ReLUs activation function and the Sigmoid activation function were compared under the same conditions. Different activation functions were tested under the condition that the network parameters are consistent with the experimental conditions. The result is shown in Figure 12.
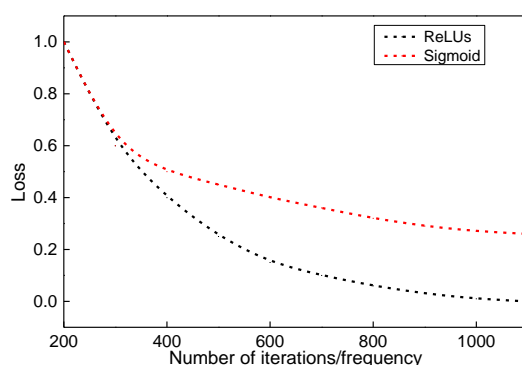

FIGURE 12. **The loss curve of the function ReLUs and Sigmoid**

Since the number of training iterations is about 1000 times, the loss curve tends to be flat, so the two activation functions of 1000 iterations are mainly analyzed. Figure 12 is the comparison result of the fine-grained prediction experiment of malignant thyroid nodules. From this figure, the loss value of the experiment using the ReLUs function as the nonlinear activation function decreases faster, the The Sigmoid function is used as the activation The loss value of the

function drops to 0.3. Therefore, the ReLUs function as the activation function has a better convergence effect. This function can appropriately remove the secondary information of the ultrasound image, reduce the amount of image feature acquisition in the deep convolutional neural network, and then reduce the network burden, increase the accuracy of network feature prediction. In this paper, the network is optimized by introducing L2 regularization and selecting the ReLUs activation function, so that the network model's ability to extract image features and the ability to organize the correlation between image features are improved.

In the experimental operation, the features of the thyroid ultrasound image will be further extracted after each convolution, and the low-level features will be obtained by extracting the features of the thyroid ultrasound image in the convolution network. This paper constructs and introduces the CNN-Fusion network in the network model. The network will first fuse the thyroid ultrasound image features and the relationship matrix between the features, and then further extract the weight matrix obtained after the fusion, through the convolutional layer and the cooling layer. The operation to achieve the acquisition from low-level features to high-level features of thyroid ultrasound images, as shown in Figure 13.
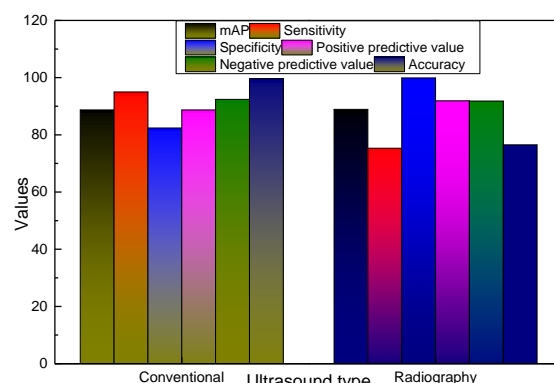

FIGURE 13. **Comparison of the accuracy of two diagnostic methods in distinguishing benign and malignant thyroid nodules**

In the experiment, L2 regularization is used, the appropriate activation function and surtax are selected, the network model is optimized, and the network performance is enhanced so that it has obvious advantages in the prediction and prediction of thyroid ultrasound images. The convolutional network is used to extract the features of the thyroid ultrasound image, and the image features that can be used to distinguish the pathology of the patient are extracted. Using the characteristics of the bidirectional propagation of the recurrent network, the network can learn according to the weight matrix obtained by the upper network processing and the input of the layer during the learning process, and the correlation between the image features in the thyroid ultrasound image is obtained through layer processing. Thyroid ultrasound image prediction process, not only uses the image feature judging category prediction image but also

uses the network learning process. The relationship between the various pathological features obtained in the database is further improved and assisted in determining the category of the predicted image.

The feature fusion network CNN-Fusion is the key part of the cyclic convolutional neural network in this article. The input of the CNN-Fusion network is the feature matrix extracted from the thyroid ultrasound image by the convolutional network and the recurrent network based on the correlation relationship between the features obtained by the thyroid ultrasound image. The feature matrix is the image feature matrix and the thyroid nodules are reproduced to a certain extent. The matrix of the relationship between clinicopathological features, the two matrices enter the Merger layer and merge into a single weight matrix, so that the weight matrix contains image characteristics and their relationships, which is more rigorous than using image features to predict and predict thyroid ultrasound images. By the above experimental analysis methods used in this paper convolution network combined with the advantages of the cycling network in accuracy, sensitivity, and specificity and other aspects of the performance is better, - given the extent of reducing the burden on the network, increase network Forecast accuracy.

V. CONCLUSION

In this paper, in the prediction of malignant thyroid nodules in ultrasound images based on deep learning algorithms, the CascadeMaskR-CNN detector is improved by effectively balancedL1loss loss function and soft-NMS method. Aiming at the problem of insufficient experimental samples, pre-trained ResNet is used to perform transfer learning. The diagnostic efficiency of the target detection model in this experiment for thyroid nodules is improved compared with the original model and is better than the current mainstream model in the field of target detection. It also has obvious advantages in comparison with the diagnostic efficiency of senior and lower-skilled physicians. The qualitative diagnosis of TI-RADS4b nodules is currently a difficult point in the TI-RADS graded diagnosis, and the complicated thyroid background will also interfere with the diagnosis of thyroid nodules. This target detection model can play a certain auxiliary role in the ultrasound diagnosis of benign and malignant thyroid nodules, but the model still has certain positioning problems in real applications. In future research, the sample size can be expanded, and it is hoped that the positioning ability of the model will be further improved. Artificial intelligence technology is growing day by day. It is believed that with the joint efforts of many medical and computer engineering researchers, artificial intelligence technology can become a powerful assistant in the protection of human health. This paper focuses on combining the advantages of convolutional neural networks and recurrent neural networks to build recurrent convolutional neural networks. This research combines the image features extracted by recurrent neural networks and

convolutional neural networks through the Merge algorithm and optimizes the prediction model. It predicted by the roof tax predictor to obtain a higher accuracy prediction result.

REFERENCES

[1] Ng CK, Wu CH, Yung KL, Ip WH, Cheung T. A semantic similarity analysis of Internet of Things[J]. Enterprise Information Systems, vol. 12, no. 7, pp. 820-855, Aug 2018.

[2] Lai CT, Jackson PR, Jiang W. Shifting paradigm of service-dominant logic via Internet-of-Things with applications in the elevators industry[J]. Journal of Management Analytics, vol. 4, no. 1, pp. 35-54, Jan 2017.

[3] British R, Najafi B, Armstrong DG. Health sensors, smart home devices, and the internet of medical things: an opportunity for dramatic improvement in care for the lower extremity complications of diabetes[J]. Journal of diabetes science and technology, vol. 12, no. 3, pp. 577-586, May 2018.

[4] Lee H, Na O, Kim Y, Chang H. A study on designing public safety service for Internet of Things environment[J]. Wireless Personal Communications, vol. 93, no. 2, pp. 447-459, Mar 2017.

[5] Serrano W. Digital systems in smart city and infrastructure: digital as a service[J]. Smart cities, vol. 1, no. 1, pp. 134-154, Dec 2018.

[6] Yuan SN, Ip HH. Using virtual reality to train emotional and social skills in children with autism spectrum disorder[J]. London journal of primary care, vol. 10, no. 4, pp. 110-112, Jul 2018.

[7] Humberside H, Dinesh K, Shishvan or, Boggio-Dandry A, Sharma G, Soyata T. A Survey of Healthcare Internet of Things (HIoT): A Clinical Perspective[J]. IEEE Internet of Things Journal, vol. 7, no. 1, pp. 53-71, Oct 2019.

[8] Elongated N. Augmented reality and virtual reality in education. Myth or reality? [J]. International Journal of Emerging Technologies in Learning (IJET). Vol. 14, no. 03, pp. 234-242, Feb 2019.

[9] Papaveraceae G, Drigas A, Skianis C, Lytras M, Papanastasiou E. Virtual and augmented reality effects on K-12, higher and tertiary education students' twenty-first century skills[J]. Virtual Reality, vol. 23, no. 4, pp. 425-436, Dec 2019.

[10] Bergman M, Willems K, Van Kerrebroeck H. Can't touch this: the impact of augmented reality versus touch and non-touch interfaces on perceived ownership[J]. Virtual Reality, vol. 23, no. 3, pp. 269-280, Sep 2019.

[11] Hanna MG, Ahmed I, nine J, Prajapati S, Pantanowitz L. Augmented reality technology using Microsoft HoloLens in anatomic pathology[J]. Archives of pathology & laboratory medicine, vol. 142, no. 5, pp. 638-644, May 2018.

[12] Tomb Dieck MC, Jung T. A theoretical model of mobile augmented reality acceptance in urban heritage tourism[J]. Current Issues in Tourism, vol. 21, no. 2, pp. 154-174, Jan 2018.

[13] Iris R, Gheisari M, Esmaeili B. par: Using augmented 360-degree panoramas of reality for construction safety training[J]. International journal of environmental research and public health, vol. 15, no. 11, pp. 2452-2452, Nov 2018.

[14] Garzón J, Pavón J, Baldiris S. Systematic review and meta-analysis of augmented reality in educational settings[J]. Virtual Reality, vol. 23, no. 4, pp. 447-459, Dec 2019.

[15] Kavanagh S, Luxton-Reilly A, Wuensche B, Plimmer B. A systematic review of Virtual reality in education[J]. Themes in Science and Technology Education, vol. 10, no. 2, pp. 85-119, Dec 2017.

[16] Gomez C, Chessa S, Fleury A, Roussos G, Preuveneers D. The internet of things for enabling smart environments: A technology-centric perspective[J]. Journal of Ambient Intelligence and Smart Environments, vol. 11, no. 1, pp. 23-43, Jan 2019.

[17] Tieri G, Morone G, Paolucci S, Iosa M. Virtual reality in cognitive and motor rehabilitation: facts, fiction, and fallacies[J]. Expert review of medical devices, vol. 15, no. 2, pp. 107-117, Feb 2018.

[18] Hughes A, Moreno A, my TH. Which destination is smarter? Application of (SA) 6 frameworks to establish a ranking of smart tourist destinations[J]. International Journal of Information Systems and Tourism (IJIST), vol. 4, no. 1, pp. 19-28, May 2019.

[19] Yang X, Lin L, Cheng PY, Yang X, Ren Y, Huang YM. Examining creativity through a virtual reality support system[J]. Educational Technology Research and Development, vol. 66, no. 5, pp. 1231-1254, Oct 2018.

[20] X. Yuan, P. He, Q. Zhu, et al., "Adversarial examples: Attacks and defenses for deep learning," *IEEE transactions on neural networks and learning systems*, vol.30, no.9, pp.2805-2824, Jan. 2019.

[21] X. Lv, D. Ming, Y. Y. Chen, et al., "very high resolution remote sensing image classification with SEEDS-CNN and scale effect analysis for superficial CNN classification," *International journal of remote sensing*, vol.40, no.2, pp.506-531, Sep. 2019.

[22] S. Zhou, Z. Xue, P. Du, "Semisupervised stacked autoloader with constraining for hypersecretion image classification," *IEEE Transactions on Geoscience and Remote Sensing*, vol.57, no.6, pp.3813-3826, Jan. 2019.

[23] X. He, Y. Chen, "Optimized input for cnn-based hypersecretion image classification using spatial transformer network," *IEEE Geoscience and Remote Sensing Letters*, vol.16, no.12, pp.1884-1888, May 2019.

[24] Boy, Nikolas, et al. "Proposed recommendations for diagnosing and managing individuals with glutaric aciduria type I: second revision." *Journal of inherited metabolic disease*, vol. 40, no.1, pp. 75-101, Sep.2017.

[25] Montagnese, Sara, et al. "Hepatic encephalopathy 2018: A clinical practice guideline by the Italian Association for the Study of the Liver (AISF)." *Digestive and Liver Disease*, vol. 51, no.2, pp. 190-205, Apr. 2019.

[26] Castello, Luigi Mario, et al. "Efficacy and safety of two different tolvaptan doses in the treatment of hyponatremia in the Emergency Department." *Internal and emergency medicine*, vol. 12, no.7, pp. 993-1001, Sep.2017.

[27] Eggers, Christian, et al. "HIV-1-associated neurocognitive disorder: epidemiology, pathogenesis, diagnosis, and treatment." *Journal of neurology*, vol. 264, no.8, pp. 1715-1727, May 2017.

[28] Hatvani, Janka, et al. "A Tensor Factorization Method for 3-D Super Resolution With Application to Dental CT." *IEEE Transactions on Medical Imaging*, vol. 38, no. 6, pp. 1524–1531, Jun. 2019.

[29] Tao, Jun, and Gang Sun. "Application of Deep Learning Based Multi-Fidelity Surrogate Model to Robust Aerodynamic Design Optimization." *Aerospace Science and Technology*, vol. 92, pp. 722–737, Jan. 2019.

[30] Qin, Qi, et al. "Algorithms for Immunochromatographic Assay: Review and Impact on Future Application." *Analyst*, vol. 144, no. 19, pp. 5659–5676, Jan. 2019.

[31] Wu, Zhuang, et al. "Application of Image Retrieval Based on Convolutional Neural Networks and Hu Invariant Moment Algorithm in Computer Telecommunications." *Computer Communications*, vol. 150, pp. 729–738, Jun. 2020.

[32] Han, Yoseob, and Jong Chul Ye. "Framing U-Net via Deep Convolutional Framelets: Application to Sparse-View CT." *IEEE Transactions on Medical Imaging*, vol. 37, no. 6, pp. 1418–1429, Oct. 2018.

[33] Guest, Dan, et al. "Deep Learning and Its Application to LHC Physics." *Annual Review of Nuclear and Particle Science*, vol. 68, no. 1, pp. 161–181, Jan. 2018.

[34] Khan, Samir, and Takehisa Yairi. "A Review on the Application of Deep Learning in System Health Management." *Mechanical Systems and Signal Processing*, vol. 107, pp. 241–265, Jun. 2018.

[35] Shah, Abhay, et al. "Multiple Surface Segmentation Using Convolution Neural Nets: Application to Retinal Layer Segmentation in OCT Images." *Biomedical Optics Express*, vol. 9, no. 9, pp. 4509–4526, Oct. 2018.

[36] Roth, Holger R., et al. "Deep Learning and Its Application to Medical Image Segmentation." *Medical Imaging Technology*, vol. 36, no. 2, pp. 63–71, May. 2018.

[37] Wei, Wei, et al. "Deep Transfer Learning for Star Cluster Classification: I. Application to the PHANGS–HST Survey." *Monthly Notices of the Royal Astronomical Society*, vol. 493, no. 3, pp. 3178–3193, Feb. 2020.

[38] Palangi, Hamid, et al. "Deep Sentence Embedding Using Long Short-Term Memory Networks: Analysis and Application to Information Retrieval." *IEEE Transactions on Audio*, Speech, and Language Processing, vol. 24, no. 4, pp. 694–707, Oct. 2016.

[39] S. Li, W. Song, L. Fang, et al., "deep learning for hypersecretion image classification: An overview," *IEEE Transactions on Geoscience and Remote Sensing*, vol.57, no.9, pp.6690-6709, Apr. 2019.

Yinghui Lu, Graduated from Zhengzhou University in 2001, is currently working in Zhumadian Central Hospital of Henan Province. Her research direction is obstetrics and Gynecology ultrasound, especially for prenatal fetal malformation screening and fetal echocardiography.

Yi Yang, Graduated from Guangzhou Medical College in June 2009, is currently working in the maternal and child health care hospital of Dongguan, Guangdong province. Her research direction is obstetrics and Gynecology, pediatric ultrasound, especially for obstetric deformity and ultrasonic diagnosis of digestive tract malformation in children.

Ling Wang, graduated from Medical College of Zhengzhou University in 2008, majored in imaging diagnosis. She has been working in the ultrasound department of Zhumadian central hospital since December 2008. She is good at superficial, obstetrics and abdominal ultrasound diagnosis.
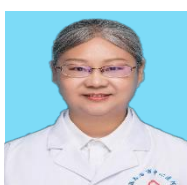
Qin Li, Graduated from Xinxiang Medical College in 2004, majored in ultrasonic medicine. She is proficient in the diagnosis of common diseases of abdomen, superficiality, obstetrics and Gynecology, especially good at prenatal four-dimensional screening of fetus and ultrasonic diagnosis of fetal echocardiography.

Wan Chen, graduated from Jinzhou Medical University of Liaoning Province in 2007, is now working in Shenzhen Hospital of Southern Medical University in Shenzhen City, Guangdong Province. At present, she is good at obstetric ultrasound examination (good at prenatal ultrasound screening and monitoring of fetus), and gynecological ultrasound examination.